Multimode interference (MMI) devices in silicon hollow waveguide technology for military electro-optic systems

R M Jenkins[*], M E McNie[**], E K Gorton[***], A F Blockley[****], and, J O Maclean[*****]
Optronics Centre, QinetiQ, St Andrews Road, Malvern, Worcestershire, U.K.,WR14 3PS.

ABSTRACT

Component alignment slots and low attenuation hollow waveguides formed in silicon substrates by standard DRIE etching techniques provide the optical analogue of the electronic printed circuit board. In conjunction with conventional pick-and-place equipment this new hybrid integration technology will facilitate low cost mass production of compact, rugged, electro-optic microsystems for military platforms. In addition to the integration of discrete components (lasers, modulators, detectors, wave-plates etc) monolithic components are also feasible. These include: (i) the analogues of free space components – plane and curved mirrors, polarization splitters, diffraction gratings, MEMS devices for beam steering etc, and, (ii) hollow waveguide components – tapers for mode matching, proximity couplers, waveguide attenuators, and, a range of multimode interference (MMI) devices. MMI devices are attractive in that they offer a wide range of optical functionality from simple geometric structures, these include intensity and wavelength splitters and mixers. In this context the military efficacy of the technology is highlighted in the demonstration of a novel form of waveguide spectrometer for a new generation of hyperspectral sensors.

Keywords: integrated optics, optical waveguides, hollow waveguides, multimode interference (MMI) devices.

1. INTRODUCTION

Hollow waveguides have been demonstrated as the basis of an integrated optic approach to 10.6μm laser radar systems [1]. As illustrated in figure 1, in such systems, 2.0 mm wide hollow waveguides formed in the surface of a polycrystalline alumina substrate were used to guide radiation through a circuit of components. The waveguides, and, deeper alignment slots for discrete components, were created by computer controlled milling techniques. A lid formed the upper wall of the hollow guides.

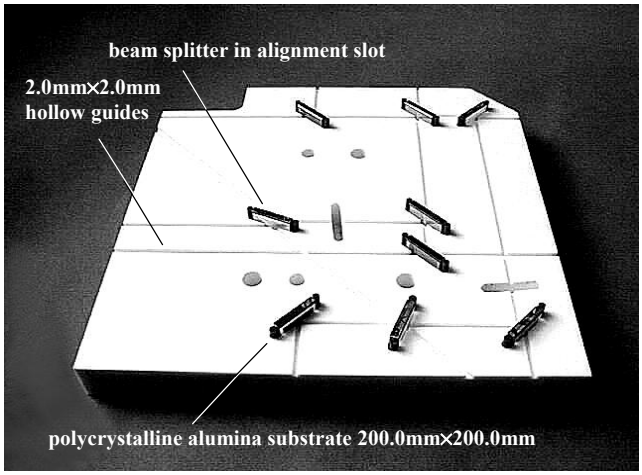

Fig.1. Photograph of a hollow waveguide based 10.6 μm lidar subsystem. The 10.6 μm radiation is guided through the circuit of components in the 2.0 mm cross-section hollow waveguides – a lid forms the forth (upper) wall of all the waveguides. The components include fully reflecting mirrors, beam splitters, Brewster plates etc.

Electro-Optical and Infrared Systems: Technology and Applications,
edited by Ronald G. Driggers, David A. Huckridge, Proc. of SPIE Vol. 5612
(SPIE, Bellingham, WA, 2004) · 0277-786X/04/$15 · doi: 10.1117/12.578252

The large cross-section and large index step associated with the hollow guides meant that they had a multimode nature. However, with appropriate lateral and angular alignment tolerances, high fidelity fundamental mode excitation and propagation was readily achieved in practice. This led to very efficient performance of the resulting subsystem [1].

As illustrated in figure 2, MEMS microfabrication techniques in conjunction with silicon substrates are being investigated for forming hollow guides, and deeper component alignment slots, in order to create a minaturized version of the concept for use in the near-IR, i.e. 1.0 – 2.0 μm [2-4]. The goal is to create the optical equivalent of the electronic printed circuit board. Standard surface mount technology can then be used for the automated manufacture of low cost hybrid modules. These include: (i) optical telecomms modules (for both fibre and free-space comms) – Tx/Rx, EDFAs, Mux/Demux, MEMS VOAs and switches etc, (ii) interferometric sensors – displacement, motion etc, (iii) gas, vapour, liquid, chemical & biological sensors – lab-on-a-chip, (iv) direct and coherent detection lidar, and, (v) a range of military micro-optical systems – including hyperspectral sensors. Hollow guides have several advantages. They exhibit low loss (< 0.1 dB/cm), broad waveband, high power, transmission characteristics and low PDL (< 0.1 dB/cm). Interfacing to free-space and fibre-based systems is simplified by less demanding lateral alignment tolerances. Compared with solid core guides, neither index matching gels, nor AR coatings, are required on the guide ends when discrete devices are integrated into the waveguide circuit.

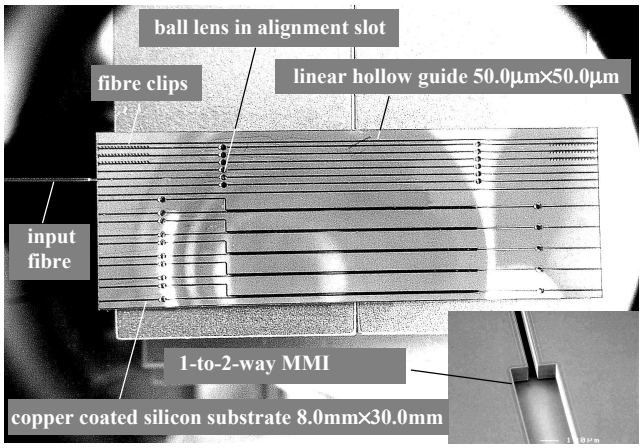

Fig.2. Photograph of 8 mm by 30 mm silicon chip including a range of monolithic hollow waveguide and integrated discrete components. On the upper left side of the chip a single mode fibre is held in position in a fibre guide with clips also formed in the DRIE process. Efficient coupling from the 9 micron core single mode fibre to the 125 micron square hollow waveguide is achieved by means of a ball lens. The lens is integrated into the surface of the chip by location in a deeper alignment slot formed in a double etch process. The chip also includes monolithic 1-to-2-way hollow waveguide MMI splitters. Lateral separation of the outputs is achieved by pairs of monolithic 45° fully reflecting mirrors in dog-leg configurations. The chip is coated with a CVD coating of copper. This minimises the attenuation coefficients as described in section 2. A copper coated lid provides the fourth, upper wall of all the waveguides.

In addition to discrete device integration, monolithic components are also feasible [1-7]. These fall into three categories, (i) analogues of free-space components - full and partial reflectors, plane or curved (for 1D field expansion or compression), Brewster windows, gratings etc. (ii) hollow waveguide components - curved guides, horns, fixed attenuators, proximity couplers, multimode interference (MMI) devices, and, (iii) MEMS (micro-electro-mechanical systems) devices, including micro-mirrors for beam steering, beam switching, and for VOAs, and, as phase shifters in hollow guide based 1-to-N-way MMI optical switches.

A prerequisite of utilizing hollow waveguides in the manner described is that they should exhibit low attenuation coefficients and low polarisation dependent loss (PDL) in the waveband of interest. This paper describes: (i) the theory and demonstration of low loss hollow waveguides, (ii) the definition of the lateral and angular alignment tolerances required to ensure high fidelity fundamental mode propagation, and, (iii) the design criteria behind, and the demonstration of, a range of MMI devices, including a novel form of waveguide spectrometer for hyperspectral sensors. We start by considering how we set about achieving low loss hollow silicon waveguides

2. POWER TRANSMISSION CHARACTERISTICS - THEORY AND MEASUREMENT

Hollow guides for optical circuit boards of the form proposed need to provide high transmission and low PDL in the waveband of interest. The power transmission of the EH_{pq}^{y} mode of a hollow rectangular guide can be written as [8]:

$$T_{pq^{y}{}_{dB}} = -4.34\,L\lambda^{2}\left[\frac{p^{2}}{w_{1}^{3}}\mathrm{Re}\left(\frac{1}{\left((n-ik)^{2}-1\right)^{1/2}}\right)+\frac{q^{2}}{w_{2}^{3}}\mathrm{Re}\left(\frac{(n-ik)^{2}}{\left((n-ik)^{2}-1\right)^{1/2}}\right)\right] \qquad (1)$$

Here L, is the length of the waveguide along the z axis; λ, is the wavelength of the radiation; p and q are integers that define the transverse nature of the mode across the x and y axes; w_1 and w_2 are the depth and width of the hollow rectangular core, and, $n - ik$, is the complex refractive index of the wall. The nomenclature EH_{pq}^{y} indicates that the mode is linearly polarised along the y-axis. In the regime where $n > 1.50$ (for all k) and n < 0.75 (for k > 0.5), the second term in the square brackets (the TM component) dominates. In this regime the fundamental mode ($p = q = 1$) power transmission of a square guide ($w_1 = w_2 = w$) simplifies to: $T_{11dB} \sim -4.34\,L\lambda^{2}n/w^{3}$. This highlights the importance of using small n and large w for low loss.

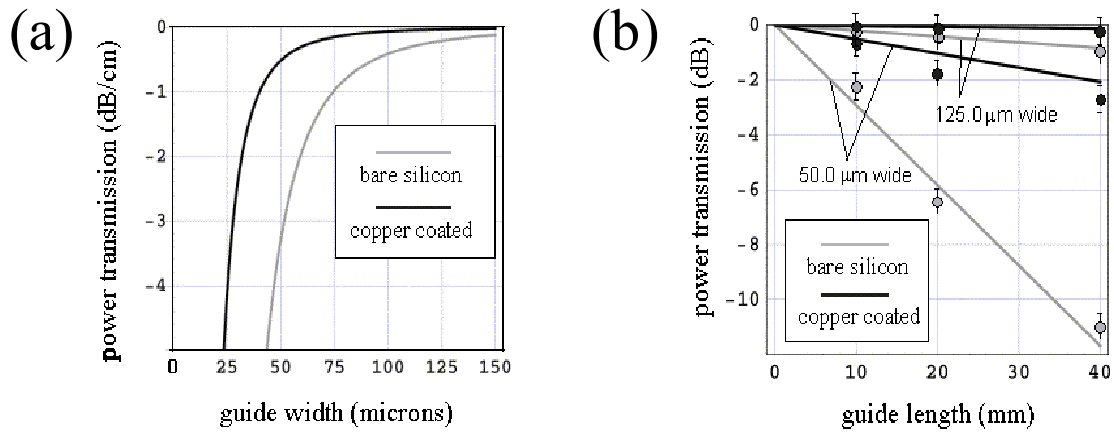

Figure 3. (a) theoretical predictions, and, (b) experimental measurements (points), of the power transmission characteristics of hollow waveguides with bare silicon (Si) walls and copper (Cu) coated walls, respectively.

Figure 3a shows predictions of the fundamental mode power transmission coefficient (dB/cm) for a square guide as a function of its width in microns. The calculations are for λ = 1550 nm for bare silicon (Si) walls (n = 3.48, k = 0.0), and, for walls having a copper (Cu) coating (n = 0.606, k = 8.26). The sub-unity value of n for Cu is due to anomalous dispersion phenomena; gold (Au) and silver (Ag) display similar characteristics around 1550 nm. Guides with width and depth tolerances better than ± 0.5 µm and $\pm 0.03w$ µm, respectively, were created using photolithography and deep reactive ion etching (DRIE) [3,4]. Equation (1) indicates that good cross-sectional symmetry is important in order to minimise polarisation dependent loss (PDL). Improved depth tolerance could be achieved with silicon-on-insulator (SOI) wafers where the buried oxide (BOX) silica layer acts as an etch stop [2-4]. The inner surfaces of the waveguides were coated with a thin film of Cu using Chemical Vapour Deposition (CVD). Sputtered or tilt-evaporated Au coatings are preferred for production [2-4]. A second wafer formed the upper wall of all the guides. Figure 3b shows the results of measurements of transmission for guides of 50.0 µm and 125.0 µm in width, both with and without Cu coatings. The results are in very good agreement with theory and emphasis the value of using large guide widths and Cu coatings in attaining low attenuation. The 125.0µm Cu coated guide provides an attenuation and a PDL < 0.1dB/cm. However, as will become clear in the next section the use of such large guide cross-sections is not without its challenges.

3. LATERAL AND ANGULAR ALIGNMENT TOLERANCE CONSIDERATIONS

The use of large guide cross-sections in conjunction with appropriate single layer metallic coatings appears to be a good approach to achieving low loss hollow waveguides. Efficient mode coupling to/from devices with smaller mode diameters (single mode fibres or solid core waveguides) is possible with ball lenses, or, in the case of fibers, ball-lensed fibres. Larger guide cross-sections also mean easier lateral alignment tolerances. However, larger guide widths also lead to tighter angular alignment tolerances. Say we want to couple to the fundamental mode of a hollow guide, or from the fundamental mode of one hollow guide to another via a transmissive or reflective component, e.g. a discrete beam splitter, a thin film filter etc. Based on overlap integral calculations, figures 4a & 4b illustrate the fundamental mode power coupling coefficient that would be achieved as a function of both lateral and angular misalignment.

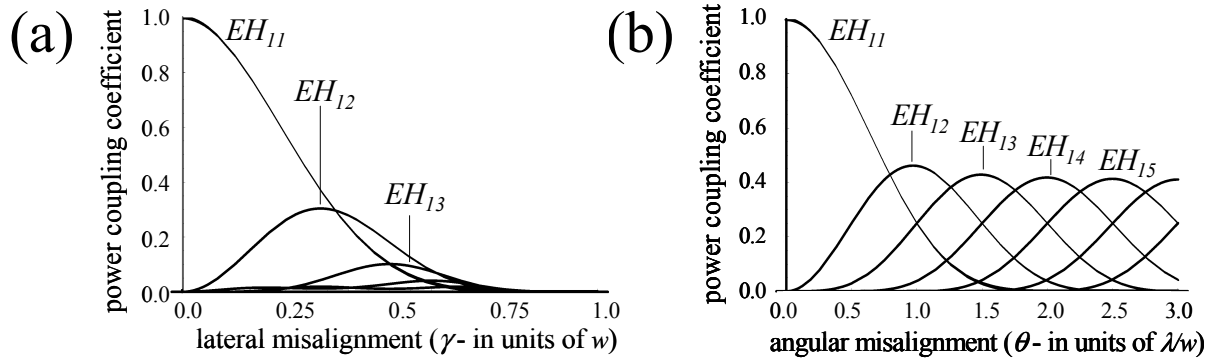

Figure 4. Predictions of fundamental mode power coupling coefficient for: (a) lateral, (b) angular, misalignment.

From figure 4, fractional power coupling coefficients of ~ 0.95 (–0.2 dB) can be achieved for lateral and angular alignment tolerances of, $\gamma \leq w/10$ *(3),* and, $\theta \leq \lambda/5w$ *(4)*, respectively. For a 50.0 μm square hollow guide and 1550 nm radiation: $\gamma \leq$ 5.0 μm, and, $\theta \leq$ 6.0 mrad (0.34°) - a 6.0 mrad angular misalignment equates to a lateral offset of 6.0 μm over 1.0 mm. If these tolerances are to be achieved by the simple location of components in alignment slots, then appropriate tolerances have to be realised on the waveguides, the alignment slots, and, the components themselves. The predictions in figures 3 and 4 highlight how the choice of guide width effects the trade-off between attenuation coefficient, lateral alignment tolerance, and, angular alignment tolerance. If smaller dimension guides are required in order to facilitate less demanding angular alignment tolerances, low insertion loss can still be achieved with multilayer wall coatings [9].

4. MULTIMODE INTERFERENCE DEVICES

As noted in the introduction, in addition to the integration of discrete components a range of monolithic devices are also possible. These fall into two main categories: (i) the analogues of free space components, and, (ii) hollow waveguide components. For the remainder of the paper we turn our attention to an important example of the latter in terms of multimode interference (MMI) devices. We start off with discussions about the design and demonstration of the basic optical functions and then address a very important spectrometer function which can provide the basis of a very compact rugged hyperspectral sensor.

4.1. Theory and demonstration of basic MMI field splitting and mixing functions

Figure 5 illustrates: (a) a schematic of the basic design configuration, (b) theoretical line profile predictions for the multimode region, (c) an SEM photograph of a hollow silicon device, and, (d) experimental results for a symmetric hollow waveguide based MMI splitter. As shown the symmetric MMI splitter simply takes the form of a single mode input guide of cross-section a coupled symmetrically into a rectangular multimode waveguide of cross-section $a \times b$.

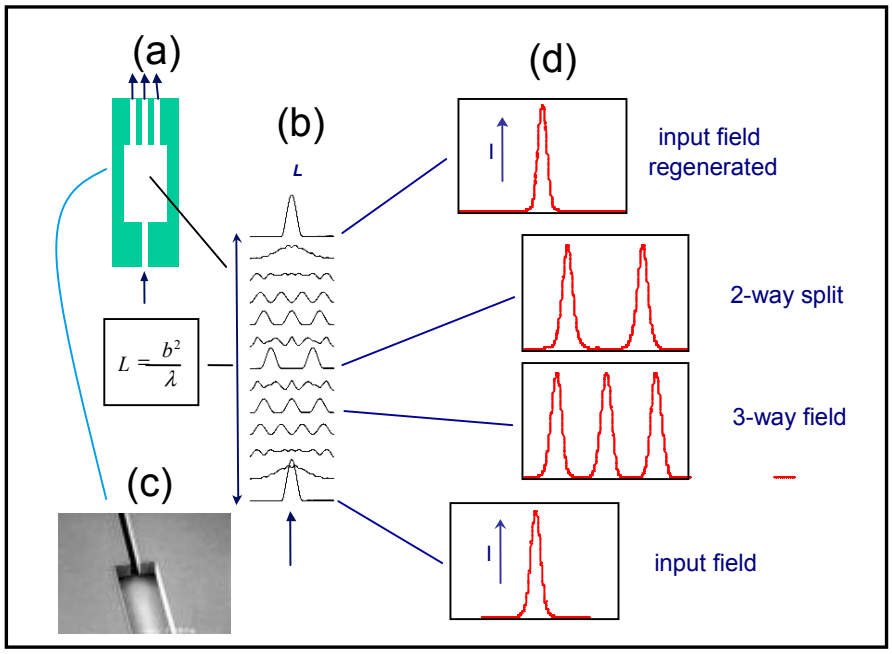

Figure 5. (a) schematic of multimode interference (MMI) splitter, (b) theoretical line-profile predictions of the field in the multimode region, (c) SEM photograph of hollow silicon MMI splitter device, and, (d) experimental results for 1550 nm input radiation and different lengths of the multimode waveguide region illustrating self-imaging of the input field and two-way and three-way splitting.

As shown in the schematic and theoretical prediction of figures 5a and 5b, for an N-way split of the input field the multimode waveguide is terminated with N output waveguides at an axial distance of $L = b^2/N\lambda$. Here λ is the free-space wavelength of the input radiation. It is interesting to note that putting $N = 1$, gives the length of multimode waveguide that produces a single self-image of the input field, i.e. $L = b^2/\lambda$. In practice, as illustrated in figures 5c and 5d, hollow waveguide multimode interference (MMI) splitters were demonstrated with a 50.0 μm square input waveguide and a 250.0 μm wide by 50.0 μm high rectangular section hollow multimode waveguide. With a multimode guide width, $b =$ 250.0 μm, and an operational wavelength of 1550 nm, a self-image of the input field occurs with a multimode guide length of $b^2/\lambda = 40.32$ mm, a two-way power split is produced at half this length, i.e., at $b^2/2\lambda$ (20.16 mm), and, a three-way power split at one third this length, $b^2/3\lambda$ (13.44 mm). In all cases the measured power attenuation was dominated by the input and output guide loss at ~0.5 dB/cm.

Figure 6 illustrates an analogous set of theoretical (figures 6a and 6c) and experimental (figures 6b and 6d) results for the case where the input waveguide is laterally offset from the axis of the multimode waveguide. This situation results in excitation of both symmetric and anti-symmetric modes in the multimode waveguide and results in self-imaging of the input field at $L = 4b^2/\lambda$, and symmetric and asymmetric splitting characteristics at $L = 4b^2/N\lambda$ and $L = 2b^2/N\lambda$, respectively. The schematic and theoretical plot in figure 6e highlight the potential of using the 1-to-2-way symmetric splitter with offset input waveguides as the basis of a coherent mixer. Depending on the relative phases of the two fundamental mode input fields, output is produced at the left-hand (as illustrated) or right-hand output guide or is shared between them. In conjunction with a semiconductor laser source and a detector, an MMI mixer of this form is under consideration as the basis of an on-chip coherent lidar system.

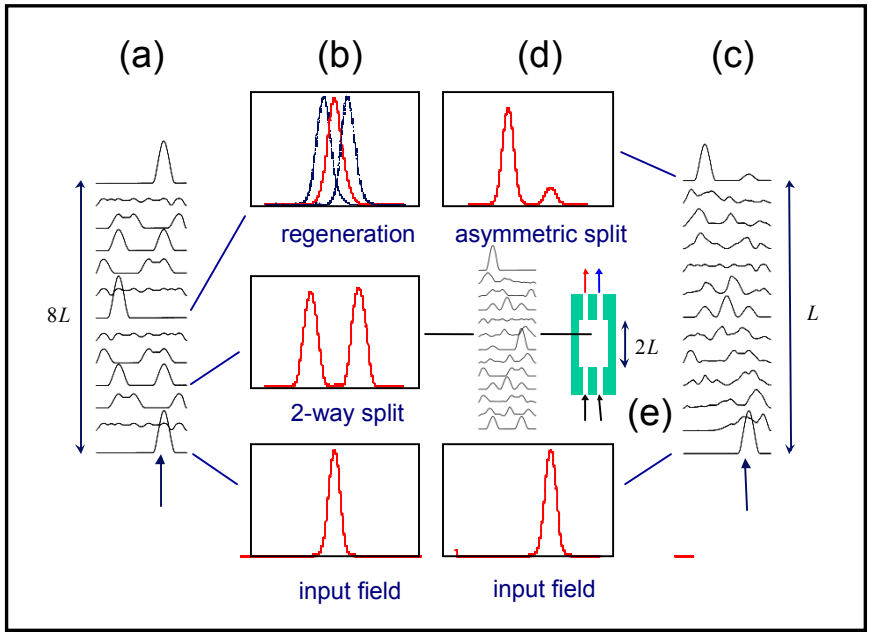

Figure 6. (a) & (c) theoretical line-profile predictions of the field in the multimode region for an offset input waveguide, (b) & (d) experimental results for 1550 nm input radiation and different lengths of the multimode waveguide region illustrating self-imaging (b) and two-way symmetric (b) and asymmetric (d) beam splitting.

The self-imaging and field splitting and mixing phenomena described above represent important monolithic building blocks for hollow silicon waveguide circuits. A particular attraction is that they can be formed at the same time and in the same etch step as the hollow waveguides themselves. Where the optical functionality achieved is appropriate this means that hollow waveguide MMI devices can take the place of discrete components. This leads to additional cost savings. A current limitation of the MMI devices is that they are relatively long. This is a consequence of the fact that the required length scales with the square of the width of the hollow multimode waveguide section. The width of the multimode waveguide is determined by the widths of the input and output guides. The choice of widths for the input and output guides is dictated by the need to keep propagation losses suitably low. In further developments of the technology it is anticipated that coating techniques of the form used to improve the power transmission characteritics of hollow core light-pipes [9] will allow the reduction of input, output and multimode guide widths, and hence, the realisation of much shorter MMI devices.

4.2. Theory and demonstration of MMI waveguide spectrometer for compact rugged hyperspectral sensors

The self-imaging phenomena described in the previous section has also been proposed as the basis of a novel form of waveguide spectrometer [10].The proposed spectrometer is based on the wavelength dependence of the self-imaging phenomena. The specific device design is illustrated in figure 7. As before it consists of a square cross-sectioned fundamental mode input waveguide of width a. This is coupled into a hollow multimode waveguide of height a and width b. However, as illustrated in figure 7. The axis of the input waveguide is laterally offset from the multimode waveguide axis by $+b/2$ (i.e. it runs through the corner of the multimode waveguide) and is tilted with respect to the multimode guide axis by an angle θ. At a suitable distance along the opposite side-wall of the multimode waveguide an array of square cross-sectioned output waveguides exist. The axes of the nearest and furthest of these are positioned at the axial points $4b^2/\lambda_{max}$ and $4b^2/\lambda_{min}$, respectively. Here λ_{max} and λ_{min} are the longest and shortest wavelengths in the spectrum to be analyzed. The output array collects the different wavelength components of the input field as a result of the wavelength dependence of the self-imaging phenomena.

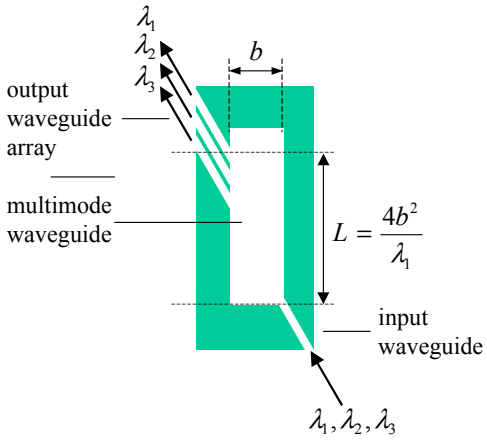

Figure 7. Schematic of optical waveguide spectrometer based on wavelength dependent self-imaging in a hollow rectangular multimode waveguide. The schematic illustrates the offset (and tilted) input waveguide, the multimode waveguide, and, the array of offset (and tilted) output waveguides. The individual output guides capture the resolved wavelength components of the input spectrum.

4.2.1. Analytical theory and numerical calculations for the MMI waveguide spectrometer

As illustrated in figure 7, where a fundamental mode input field from a square cross-section input guide enters a rectangular guide of the same height but different width, only modes of order EH_{1q} are excited. Within the paraxial approximation (i.e. $(\lambda/2a)^2 + (q\lambda/2b)^2 << 1$) it can be shown [11], as noted previously, that a self-image (strictly speaking a mirror image) of the input field is produced at an axial distance:

$$L = 4\frac{b^2}{\lambda} \qquad (2)$$

Differentiation of equation (2) with respect to wavelength gives the incremental shift, dL, in the axial position of the self-imaging point for an incremental change in wavelength, $d\lambda$, as:

$$dL = -4\left(\frac{b}{\lambda}\right)^2 d\lambda \qquad (3)$$

In order to provide a better insight into the way that the waveguide spectrometer would operate in practice, numerical calculations have been used to predict the transverse intensity contours that are produced in a rectangular cross-section multimode waveguide. The calculations are based on the excitation and propagation of an appropriate spectrum of modes in the the multimode waveguide. In this context it was assumed that: (i) the multimode waveguide had vertical side walls, (ii) that the excited modes had pure sinusoidal form and were confined to the core region, and, (iii) that all the excited modes were lossless. On this basis a typical set of results is illustrated in figure 8 for the case of a 10.0 μm square input waveguide and a 10.0 μm high, 40.0 μm wide, multimode waveguide. The plot on the lefthand side of figure 8 shows the field intensity contour in the input region of the multimode waveguide assuming that the fundamental mode input field is tilted at an angle of 0.1 rad with respect to the multimode guide axis. On the righthand side of figure 8 are three plots showing the field intensity contours in the output region of the multimode guide for input wavelengths of 1500 nm, 1520 nm and 1540 nm, respectively. The predictions clearly indicate that there is an axial shift in the point on the left-hand wall where the self-image of the input field occurs as the wavelength of the input field changes.

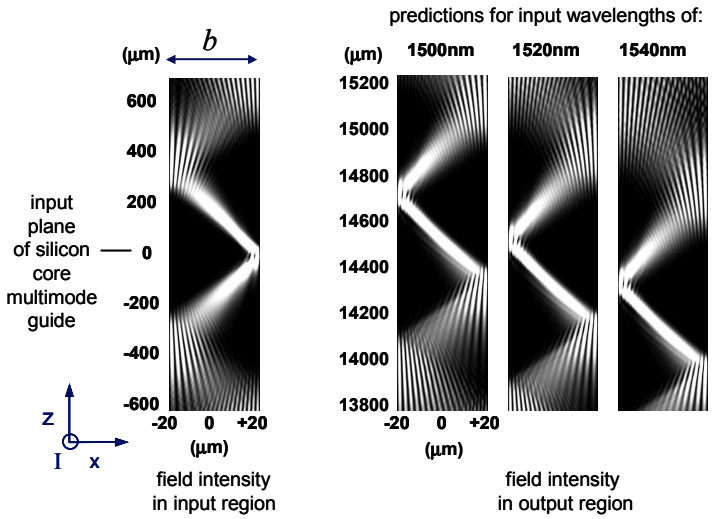

Figure 8. Left-hand side - predicted transverse intensity pattern in the input region of the multimode waveguide. Right-hand side - predicted transverse intensity pattern in the output region of the multimode waveguide, illustrating the axial shift in the self-image of the input field as a function of the change in wavelength from 1500 nm to 1540 nm in 20 nm steps.

4.2.2. Experimental demonstration of the MMI waveguide spectrometer

An experimental demonstration of the device was undertaken with a waveguide structure of the form illustrated schematically in figure 7. In practice the hollow input and output waveguides were 25 μm square and the multimode guide was 25 μm high and 100 μm wide. The axis of the input guide was offset from the multimode guide axis by 50 μm and tilted by 0.15 rad to it. The axes of the five output guides were also tilted by 0.15 rad with respect to the multimode guide axis. On the mask design, the spectrometer devices were orientated such that the axes of the input and output guides were orthogonal to the ends of the chips. From this perspective the output guides were on a 50 μm pitch. Because of the 0.15 rad tilt of the output guides, this equates to a pitch of ~ 50/0.15 = 333 μm at the side-wall of the multimode guide. Substituting this value for dL in equation (3) along with values of 1535 nm for λ (the design wavelength for the central guide in the output array) and 100 μm for b, the predicted change in wavelength, $d\lambda$, to shift the self-imaging point from one output guide to the next is ~ 333.(1.535/100)^2/4 = 19.6 nm.

A microscope objective was used to couple the output from a tuneable laser source into the fundamental mode of the input guide. The achievement of efficient power coupling to the fundamental mode involved creating a TEM_{00} beam having a waist diameter of 0.7a at the entrance plane of the input waveguide. A second microscope objective was used to produce a magnified image of the output array on a vidicon camera. As illustrated in figure 9, line profiles were extracted from the vidicon camera for wavelengths of 1480 nm, 1500 nm and 1520 nm, as the laser was tuned from 1480 nm to 1580 nm. The 20 nm change in wavelength required to shift the light from one output guide to the next is in good agreement with the theoretical predictions based on equation (3). Because of small design and processing errors the central output guide equated to a wavelength of 1480 nm not 1535 nm as planned. As a consequence a laser source providing outputs at 1460 nm and 1440 nm would have been required to demonstrate efficient coupling to the two remaining output guides of the spectrometer device. These relate to output positions at 100 μm and 50 μm on the left of figure 9. Nevertheless, the prototype device provided effective proof of the underlying concept.

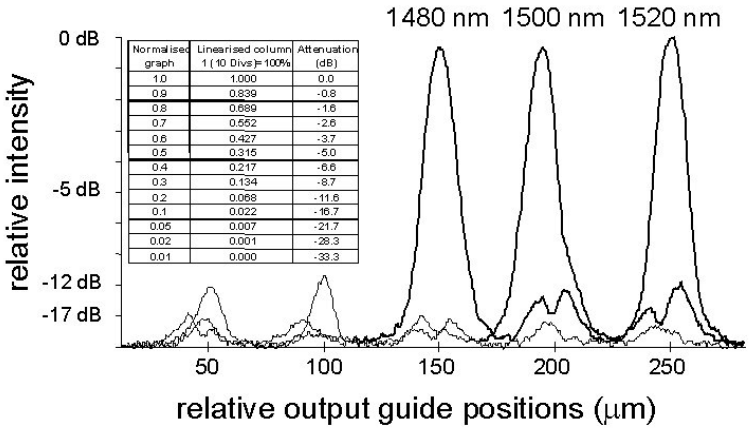

Normalised graph	Linearised column 1 (10 Divs)= 100%	Attenuation (dB)
1.0	1.000	0.0
0.9	0.839	-0.8
0.8	0.689	-1.6
0.7	0.552	-2.6
0.6	0.427	-3.7
0.5	0.315	-5.0
0.4	0.217	-6.6
0.3	0.134	-8.7
0.2	0.068	-11.6
0.1	0.022	-16.7
0.05	0.007	-21.7
0.02	0.001	-28.3
0.01	0.000	-33.3

Figure 9. Experimental measurements of the line profile outputs from the hollow waveguide MMI self-imaging spectrometer device for wavelengths 1480 nm, 1500 nm and 1520 nm . The 50 μm lateral shift in the self-image for a 20 nm change in wavelength is in good agreement with predictions based on equation (3).

5. CONCLUSIONS

Hollow waveguide integrated optic tcehnology realised in silicon substrates by means of deep reactive ion etchning (DRIE) can provide the basis of a fundamentally new approach to the hybrid integration of discrete components. In conjunction with conventional pick-and-place equipment this new hybrid integration technology should facilitate low cost mass production of compact, rugged, electro-optic microsystems for military platforms. In addition to the integration of discrete components a wide range of monolithic components are also feasible. Multimode interference (MMI) devices form an important subset of monolithic components. As described in this paper the MMI devices can provide a very wide range of intensity and wavelength splitting and recombination functions in simple hollow waveguide geometries. In particular a novel form of waveguide spectrometer based on the wavelength dependent self-imaging properties of a rectangular hollow multimode waveguide has been proposed and demonstrated. Improved resolution and bandwidth, and, reduced cross-talk and attenuation are predicted for optimised designs. MMI spectrometer devices of this form should provide an important basis for compact, rugged, low cost hyperspectral sensors.

REFERENCES

1. R M Jenkins, R W J Devereux and A F Blockley, “Hollow Waveguide Integrated Optics: a novel approach to 10.6μm laser radar,” Jn. Mod. Opt. 45, pp1613, 1998.
2. R M Jenkins, M E McNie, Patent Application GB2003/000331, priority date 29th January 2002.
3. R M Jenkins, M E McNie, A F Blockley, N Price, J McQuillan, “Hollow waveguides for integrated optics,” Proc. European Conference on Optical Communications (ECOC), Paper Tu.1.2.4, Rimini (Italy), Sept. 2003.
4. M E McNie, R M Jenkins and A F Blockley, ”Hollow waveguides - applicability to optical MEMS,” MicroTech 2004, Cambridge, UK.
5. T Miura, F Koyama, Y Aoki, A Matsutani, and, K Iga, ”Propagation characteritics of hollow waveguides for temperature insensitive photonic integrated circuits, Jpn. J. Appl. Phys. 40, pp.688, 2001.
6. T Miura and F Koyama, ECOC 2002, paper 4.4.4, Copenhagen, Denmark, September 2002.
7. T Miura, M Ishikawa, A Matsutani, F Koyama, ”Hollow waveguide with air core for tuneable planar waveguide device,” ECOC 2003, paper Tu.1.2.3, Rimini, Italy, September 2003.
8. E A J Marcatili, Bell Systems Technology Journal 48, pp2103, 1969.
9. J A Harrington, ”A review of IR transmitting hollow waveguides,” Jn Fibre and Integrated Optics, 19, pp211, 2000.

10. R M Jenkins, UK Patent Application GB2002/004560, filed 8th October 2002.
11. R Ulrich, Optics Comm. 13, 25, 1975.

* rmjenkins@qinetiq.com; phone 44 1684 894000
** memcnie@qinetiq.com; phone 44 1684 894000
*** ekgorton@qinetiq.com; phone 44 1684 894000
**** afblockley@qinetiq.com; phone 44 1684 894000
***** jomaclean@qinetiq.com; phone 44 1684 894000